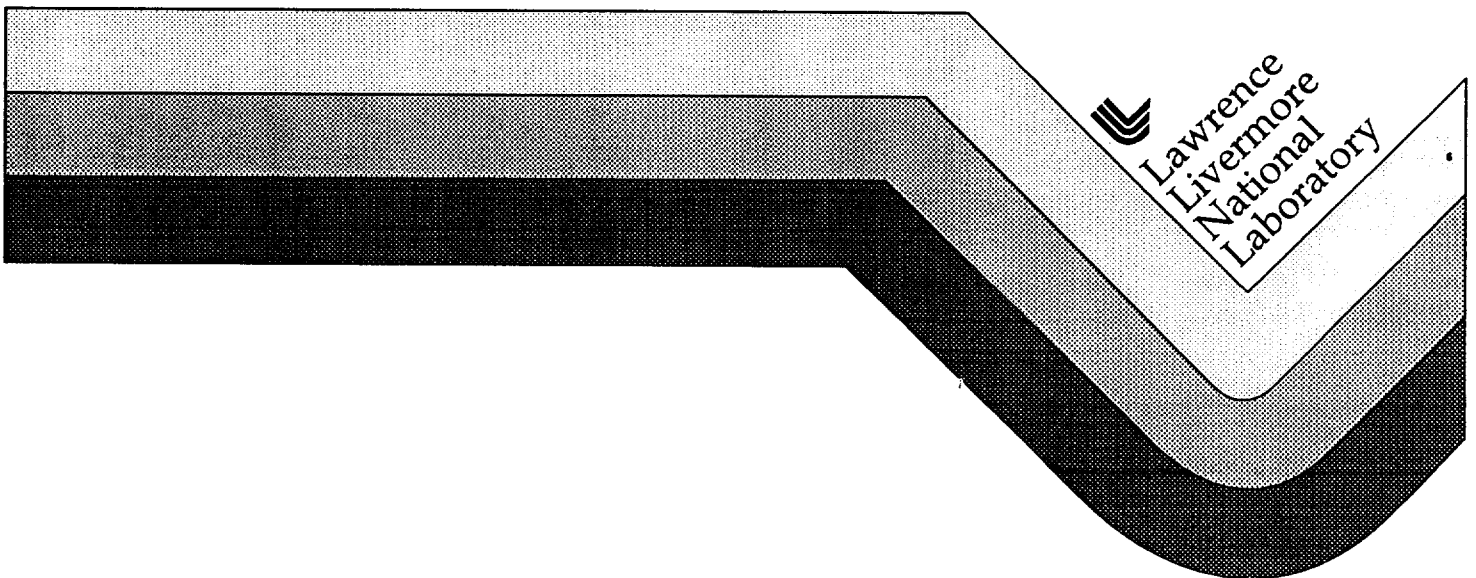


UCRL-CR-125216
S/C- 923-003

Precise Measurements of Hyperfine Components in the Spectrum of Molecular Iodine

C. J. Sansonetti

May 23, 1996



DISCLAIMER

This document was prepared as an account of work sponsored by an agency of the United States Government. Neither the United States Government nor the University of California nor any of their employees, makes any warranty, express or implied, or assumes any legal liability or responsibility for the accuracy, completeness, or usefulness of any information, apparatus, product, or process disclosed, or represents that its use would not infringe privately owned rights. Reference herein to any specific commercial product, process, or service by trade name, trademark, manufacturer, or otherwise, does not necessarily constitute or imply its endorsement, recommendation, or favoring by the United States Government or the University of California. The views and opinions of authors expressed herein do not necessarily state or reflect those of the United States Government or the University of California, and shall not be used for advertising or product endorsement purposes.

Precise Measurements of Hyperfine Components
in the Spectrum of Molecular Iodine

Craig J. Sansonetti

National Institute of Standards and Technology
Gaithersburg, MD 20899

May 23, 1996

Absolute wave numbers with a typical uncertainty of 1 MHz (95% confidence) have been measured for 102 hyperfine-structure components of $^{127}\text{I}_2$. The data cover the range 560 to 656 nm with no gaps larger than 50 cm^{-1} . The spectra were observed by using Doppler-free frequency modulation spectroscopy with a tunable cw laser. The laser was locked to selected iodine components, and its wave number was measured with a high precision Fabry-Perot wavemeter. The accuracy of the results is confirmed by the good agreement of 9 of the lines with previous results from other laboratories. These measurements provide a well-distributed set of precise reference lines for this spectral region.

INTRODUCTION

Absorption lines of molecular iodine (I_2) provide one of the most convenient sources of wavelength standards for laser spectroscopy. The entire range of the I_2 B-X band system has been studied at high resolution by Fourier transform spectroscopy and presented in an atlas by Gerstenkorn and Luc.¹ With a small correction presented in a later paper,² the atlas wave numbers provide a dense comb of standards covering the green to red portions of the spectrum with an accuracy of about 0.002 cm^{-1} . This relative accuracy, about a part in 10^7 , is satisfactory for calibration of spectra recorded with broadband lasers or by classical methods. But for precise measurements with stable single-frequency lasers, standards of higher accuracy are needed.

The Doppler-limited I_2 absorption spectrum is not suitable for use as a standard at higher accuracy because its line profiles have varying asymmetries that reflect underlying hyperfine structure. Each iodine line is a composite of 15 or 21 hyperfine components that cannot be resolved using classical methods. By Doppler-free laser spectroscopy, however, these components can be fully resolved and used as well-defined reference lines. Notable cases in point are the lines used to stabilize He-Ne lasers at 633 and 612 nm and the argon ion laser at 514 nm.³

A number of groups have made precise measurements of selected iodine lines for calibration purposes in particular experiments. The largest group of lines (27) was reported by Hlousek and Fairbank⁴ in connection with their measurements of Doppler-free two-photon and saturated-absorption lines in helium. Most of their iodine lines, however, were measured with only modest accuracy (0.0002 cm^{-1}). A few lines have been reported by other groups with much higher accuracy.^{5,6,7}

Over the past decade hyperfine components in 102 I₂ lines spanning the range from 560 to 656 nm have been measured in our laboratory at NIST. The accuracy of the results is generally about 2 parts in 10⁹. Coverage of this spectral region (15233 to 17845 cm⁻¹) is fairly uniform. There are no gaps wider than 50 cm⁻¹. In this paper we present all of our Doppler-free iodine measurements. The results should be useful to other workers who need high-accuracy reference wavelengths in this spectral region.

EXPERIMENT

Because this paper represents a collection of data measured in a number of experiments over a period of nearly ten years, not all of the measurements were made under identical experimental conditions. Almost all of the observations reported here have been made using Doppler-free frequency modulation (FM) spectroscopy, although some of the earliest measurements employed a simple saturated absorption setup with a frequency dither imposed on the tunable dye laser for locking to the iodine lines. Since the observed wave numbers do not depend on the exact Doppler-free technique employed, we will not discuss the variations in technique that may apply to some of the measurements. The experimental apparatus and methods described here are representative of those used for most of the data.

Our technique for observing Doppler-free spectra of I₂ lines by FM spectroscopy is essentially similar to that described by Hall, Holberg, Baer, and Robinson.⁸ The theory of FM spectroscopy including a detailed analysis of the observed line shapes has been presented by Bjorklund, Levenson, Lenth, and Ortiz.⁹

Apparatus typical of that used in these measurements is shown in Figs. 1 and 2. A commercial ring dye laser operated with the dyes Rhodamine 6G, DCM, or Rhodamine 110 provides tunable single-frequency radiation with a line width of less than 1 MHz. The laser beam is split into a strong saturating beam and a weak probe beam that counterpropagate coaxially through the iodine cell. The beams in the cell are 2 mm in diameter and approximately collimated. The frequency of the saturating beam is shifted upward by 72 MHz and its intensity is sinusoidally modulated at 85 kHz by an acousto-optic modulator (AOM). The frequency shift introduced by the AOM prevents optical feedback from the counterpropagating beams into the dye laser. A variable attenuator provides for adjustment of the power in the saturating beam.

The probe beam passes through a travelling wave electro-optic phase modulator (EOM) that imposes symmetric sidebands about the laser center frequency. The sideband spacing is variable but is usually set to about the width of the transition to be observed. For I_2 a spacing of 5 to 6 MHz is used. The EOM drive power is adjusted to put 10% of the total laser power in each sideband by observing the spectrum of the probe beam on a 300 MHz optical spectrum analyzer. As the laser frequency is scanned across the transition of interest the sidebands probe the narrow saturated absorption resonance induced by the saturating beam.

After passing through the I_2 cell a portion of the probe beam intensity is diverted by a beam splitter and focused on a fast photodiode. The resulting signal is processed by a high-pass filter, double-balanced mixer, and lockin amplifier to recover the anti-symmetric FM resonance (Figure 2). The phase of the local oscillator signal to the mixer is adjusted by a variable delay line to obtain an FM signal proportional to either the dispersion of the iodine hyperfine component

(profile S_2 in Fig. 3 of Ref. 9) or its absorption (profile S_1). The dispersion profile is generally preferred because it has a steep zero crossing that is independent of the relative sizes of the line width and the sideband spacing and is very suitable for locking the laser to the iodine line. In some of our early FM measurements the absorption phase was used because at that time we could observe it with better signal-to-noise ratio.

The iodine cell used in this work was fabricated at NIST. The methods used in preparing the cell were identical to those used in making cells for I_2 -stabilized lasers constructed at NIST.¹⁰ Previous tests with such cells have shown that frequency shifts due to residual background gas pressure are less than 1 part in 10^{11} . The cell is 12 mm in diameter and 30 cm long with fused silica Brewster windows and a small sidearm. For all of our measurements the cell was operated in ambient laboratory air at a temperature of $23 \pm 1^\circ\text{C}$. At this temperature our long cell and collinear beam geometry gave excellent signal-to-noise ratio even for transitions below 16000 cm^{-1} for which heated cells are sometimes required.

Lines for measurement were initially chosen by reference to the iodine atlas of Gerstenkorn and Luc.¹ In general we tried to choose lines that were narrow and relatively isolated to reduce the likelihood of blended transitions and to make it easier to find the correct line for later use. The laser was tuned to the line of interest by using a travelling Michelson wavemeter with an accuracy of about 0.002 cm^{-1} . For each line we first made a broadband scan (about 0.045 cm^{-1} wide) to observe the hyperfine structure and to identify a hyperfine component suitable for locking the dye laser. Lines with strong overlapping components from other transitions were normally rejected because of the difficulty of routinely identifying the correct component.

After an appropriate hyperfine component had been selected, the dye laser was servo-locked to the zero crossing of its FM signal. The servo-lock was implemented by using the external scan input of the dye laser controller. It was able to maintain lock for an indefinite period, combining the long term stability of the I_2 resonance with the narrow line width of the commercial laser.

The absolute measurement of the dye laser wave number was made by using the Fabry-Perot wavemeter developed in our laboratory.¹¹ This wavemeter has been used for numerous precise measurements and has demonstrated its ability to make reliable absolute measurements at a sub-MHz level of accuracy. Measurements with the wavemeter are made with respect to a He-Ne laser stabilized to the g component of the $^{127}I_2$ transition R(127) 11-5. Our laser follows the same design as that used by Jennings *et al.*¹² who determined the frequency of this line to be 473 612 340.492 (74) MHz.

Almost all of the lines reported here were measured with both 218-mm and 7-mm Fabry-Perot spacers. Some lines were also measured with a 31-mm spacer. Results derived from observations with different spacer lengths were used to correct for phase dispersion on reflection from the coatings of the interferometer plates as previously described.¹³ The phase correction used in this work was calculated from a polynomial fit to all of our phase dispersion data from this and other experiments spanning the region 471 to 765 nm. Measuring each line with spacers of different lengths also provides assurance that the correct integer order of interference has been used in calculating the wave number.

RESULTS

The results for all I_2 lines observed in this work are collected in Table 1. For each line the Doppler-limited wave number as measured by Fourier

transform spectroscopy is given in the first column. This value can be used to locate the line in the iodine atlas of Gerstenkorn and Luc.¹

The line classifications given in the second column of Table 1 have been determined from calculations of the I₂ B-X band system made with Dunham parameters derived from the Fourier transform spectra.¹⁴ In general the I₂ spectrum is very dense, with several transitions predicted within the Doppler profile of each line listed in the iodine atlas. The classification given in the table applies to the transition for which the resolved hyperfine component was measured. It is based on the wave number, hyperfine structure, and expected intensity of the line. Other transitions not listed may also contribute to the Doppler-broadened line. We found that three lines (16339.7 cm⁻¹, 17016.1 cm⁻¹ and 17049.2 cm⁻¹) are misidentified in Ref. 4. Corrected classifications for these lines are given in Table 1.

In the third column of Table 1 we list the hyperfine component that was measured for each line. There are 15 hyperfine components for lines with even J and 21 components for lines with odd J. This hyperfine structure was explained by Kroll¹⁵ as due primarily to the nuclear electric quadrupole interaction. Kroll points out that for high J the hyperfine components appear in six distinct groups as seen in Figs. 3 and 4. Most of our lines display this common pattern. For low J, magnetic and second order electric quadrupole interactions become increasingly significant, and the distribution of components deviates from this pattern (Fig. 5).

In previous work there has been no standard convention for the labeling of the iodine hyperfine components. This has resulted in some confusion in their use. In this paper we use labels for the components as given by Gerstenkorn and Luc.² This labeling is illustrated in Figs. 3 and 4. Note that for both 15- and 21-

component lines the component labeled *o* by Hlousek and Fairbank⁴ corresponds to our component *t*.

For most lines we have chosen to measure the *t* hyperfine component. This component is convenient because it is easy to locate even if one has no precise way of measuring the wavelength of a tunable laser. First, the correct iodine line is identified by comparing the Doppler-limited laser absorption (or fluorescence) spectrum with the spectrum in the iodine atlas.¹ Then the laser is tuned onto the line from the low wave number side while observing the Doppler-free spectrum. For 15-component structures (Fig. 3) the *t* component is the first one encountered; for 21-component structures (Fig. 4) it is the central component of the first group of three.

In the fourth column of the Table 1 we present the measured wave number of the specified component and its uncertainty. The value reported is the average of 2 to 9 independent measurements made on different days with the 218-mm Fabry-Perot spacer. Each of these independent measurements is the average of about 80 successive readings from the Fabry-Perot wavemeter taken over a period of about a minute.

The uncertainty at the one standard deviation level is derived as the quadrature sum of the standard error of the mean of the individual determinations (typically about $1 \times 10^{-5} \text{ cm}^{-1}$), the estimated uncertainty of the lock point due to line asymmetry and baseline shifts ($6 \times 10^{-6} \text{ cm}^{-1}$), the uncertainty of the phase shift correction ($6 \times 10^{-6} \text{ cm}^{-1}$), the uncertainty of the reference laser wave number ($2.3 \times 10^{-6} \text{ cm}^{-1}$), and the uncertainty in the correction for the reference laser power and temperature ($2.8 \times 10^{-6} \text{ cm}^{-1}$). The uncertainty reported in Table 1 is two standard deviations and represents a 95% confidence level.

To assist in identifying the correct line and component for each measured transition, descriptive comments are included in the final column of Table 1. The first comment line describes the number and distribution of hyperfine components. In most cases the observed hyperfine components fall in six clearly defined groups. The code W is used to indicate the few lines with low J for which the components are fully resolved but distributed in such a way that these normal groupings are not apparent. For lines in which overlapping hyperfine components from other transitions are observed, additional comment lines are added that describe the interfering transitions. These comments can be understood by comparing the tabulated information for the line at 16254 cm^{-1} to the spectrum for this line which is reproduced in Fig. 5.

DISCUSSION

Our current results are compared with some previously reported measurements in Fig. 6. For clarity not all previous measurements are included. We have chosen to compare with results of Hlousek and Fairbank⁴ and of Shiner *et al.*⁶ because they have the most lines in common with this work. We also compare to three lines recommended by the Comité Consultatif pour la Définition du Mètre (CCDM).³ These three values represent the combined measurements of several laboratories and should be the most reliable absolute measurements in I_2 .

The comparison in Fig. 6 shows excellent agreement between the various measurements. All values are consistent within their quoted uncertainties with the exception of the 17030-cm^{-1} line. For this line it appears that the result of Hlousek and Fairbank⁴ is in error. Difficulty with this line is confirmed by experimental work at the Free University of Amsterdam, where the value of Hlousek and Fairbank was found to be inconsistent with other reference lines.¹⁶

It is apparent from Fig. 6 that the wave numbers measured in the present work are slightly smaller than those measured in other laboratories. With respect to the CCDM recommended values, this offset is nearly constant at an average of -210 ± 30 kHz. The offset from Shiner *et al.* has a greater scatter and averages -277 ± 146 kHz. These differences are much smaller than our estimated uncertainty but are nevertheless of some concern.

To investigate this problem we have compared the frequency of our I₂-stabilized reference laser with a second I₂-stabilized laser. The frequency of the laser used for our present measurements was found to be slightly higher than that of the comparison laser. In four determinations with realignment of the laser cavity the offset ranged from 14 to 45 kHz. This is a relative difference of about 9 parts in 10^{-11} , well within the reported uncertainty of the reference laser frequency and in the wrong direction to explain our difference with other laboratories. We have also done tests in which we measured the same iodine line using different AOM frequencies, locking the reference laser to different iodine components, and inverting the phase in the FM detection electronics. None of these tests showed a systematic effect that might contribute to the observed difference.

In Fig. 7 our present results are compared to the 19 lines measured with lower precision by Hlousek and Fairbank.⁴ Again the agreement is satisfactory. Although the measurements seem to diverge with increasing wave number, all of the values agree well within the 6 MHz uncertainty of Ref. 4. For these lines our present results are more accurate than the previous values by a factor of about 6.

In summary we have established accurate reference wave numbers for 102 Doppler-free hyperfine components in ¹²⁷I₂. These lines cover the range from 560 to 656 nm (15233 to 17845 cm⁻¹) with no gaps wider than 50 cm⁻¹. For most of the

lines the absolute accuracy is better than 1 MHz (95% confidence interval). These results should be useful as reference lines for laser spectroscopy and for calibration of wavemeters and interferometers.

ACKNOWLEDGMENTS

The help of Kevin J. Coakley of the NIST Statistical Engineering Division, who analyzed our phase dispersion data by using a statistical bootstrap procedure to obtain a globally optimized phase correction function, is gratefully acknowledged. The author also wishes to thank Howard Layer for filling the iodine cell used in this work and John Gillaspay for helpful discussions concerning Doppler-free FM spectroscopy.

Portions of this work were sponsored by Lawrence Livermore National Laboratory under contract #923-003.

References

1. S. Gerstenkorn and P. Luc, "Atlas du Spectra D'Absorption de la Molecule D'Iode," (editions du Centre National de la Research Scientifique, 15 quai Anatole-France, 75700 Paris, 1978).
2. S. Gerstenkorn and P. Luc, "Absolute iodine (I_2) standards measured by means of Fourier transform spectroscopy," *Revue Phys. App.* **14**, 791-794 (1979).
3. T. J. Quinn, "Mise en Pratique of the Definition of the Metre (1992)," *Metrologia* **30**, 523-541 (1993).
4. L. Hlousek and W. M. Fairbank, Jr., "High-accuracy wave-number measurements in molecular iodine," *Opt. Lett.* **8**, 322-323 (1983).
5. P. Juncar, J. Pinard, J. Hamon, and A. Chartier, "Absolute determination of the Wavelengths of the Sodium D_1 and D_2 Lines by Using a CW Tunable Dye Laser Stabilized on Iodine," *Metrologia* **17**, 77-79 (1981).
6. D. Shiner, J. M. Gilligan, B. M. Cook, and W. Lichten, " H_2 , D_2 , and HD ionization potentials by accurate calibration of several iodine lines," *Phys. Rev. A* **47**, 4042-4045 (1993).
7. R. Grieser, G. Bönsch, S. Dickopf, G. Huber, R. Klein, P. Merz, A. Nicolaus, and H. Schnatz, "Precision measurement of two iodine lines at 585 nm and 549 nm," *Z. für Phys. A* **342**, 147-150 (1994).

8. J. L. Hall, L. Hollberg, T. Baer, and H. G. Robinson, "Optical heterodyne saturation spectroscopy," *Appl. Phys. Lett.* **39**, 680-682 (1981).
9. G. C. Bjorklund, M. D. Levenson, W. Lenth, and C. Ortiz, "Frequency Modulation (FM) Spectroscopy," *Appl. Phys. B* **32**, 145-152 (1983).
10. H. P. Layer, "A Portable Iodine Stabilized Helium-Neon Laser, " *IEEE Trans. Inst. Meas.* **IM-29**, 358-361 (1980).
11. C. J. Sansonetti, in *Advances in Laser Science - IV*, edited by J. L. Gole, D. F. Heller, M. Lapp, and W. C. Stwalley (AIP, New York, 1988), pp. 548-553.
12. D. A. Jennings, C. R. Pollock, F. R. Petersen, R. E. Drullinger, K. M. Evenson, J. S. Wells, J. L. Hall, and H. P. Layer, "Direct frequency measurement of the I₂-stabilized He-Ne 473-THz (633-nm) laser," *Opt. Lett.* **8**, 136-138 (1983).
13. J. D. Gillaspy and C. J. Sansonetti, "Absolute wavelength determinations in molecular tellurium: new reference lines for precision laser spectroscopy," *J. Opt. Soc. Am. B* **8**, 2414-2419 (1991).
14. S. Gerstenkorn and P. Luc, "Description of the absorption spectrum of iodine recorded by means of Fourier Transform Spectroscopy: the (B-X) system," *J. Physique* **46**, 867-881 (1985).
15. M. Kroll, "Hyperfine Structure of the Visible Molecular-Iodine Absorption Spectrum," *Phys. Rev. Lett.* **23**, 631-633 (1969).

16. W. Ubachs, private communication (1995).

Figure Captions

Fig. 1. Experimental apparatus for observation of Doppler-free absorption lines in molecular iodine.

Fig. 2. Signal processing schematic for FM spectroscopy and laser locking to iodine resonances.

Fig. 3. Spectrum of the transition P80 (15-2) at 16917 cm^{-1} , a typical 15 component hyperfine structure.

Fig. 4. Spectrum of the transition R47 (9-3) at 16130 cm^{-1} , a typical 21 component hyperfine structure.

Fig. 5. Overlapping hyperfine structures at 16254 cm^{-1} which illustrate the codes used in the comments of Table 1.

Fig. 6. Deviations of previous precise measurements from the present results (previous measurement – this work). The shaded area for each line represents the uncertainty of the present results.

Fig.7. Deviations of the lines measured with lower precision by Hlousek and Fairbank⁴ from the present results. The uncertainty of of Hlousek and Fairbank is 6 MHz. The typical uncertainty for the present work is 1 MHz, indicated by the shaded region in the figure.

Table 1. Measured Wave Numbers of Hyperfine Components in I₂.

Atlas Wave Number ^a (cm ⁻¹)	Transition	Component	Measured Wave Number ^b (cm ⁻¹)	Comments ^c
15233.3653	R73 (5-5)	<i>i</i>	15233.367441 (21)	21 U (<i>p,q</i>)
15278.5914	P110 (6-5)	<i>t</i>	15278.574318 (20)	15 U (<i>d,e</i>) (<i>f,g</i>) (<i>p,q</i>)
15297.7275	P100 (6-5)	<i>t</i>	15297.712483 (24)	15 U (<i>d,e</i>) (<i>f,g</i>) (<i>p,q</i>) P149 (7-5) -790 MHz 15%
15341.8700	P72 (6-5)	<i>t</i>	15341.853034 (23)	15 U (<i>d,e</i>) (<i>f,g</i>)
15379.2371	R41 (6-5)	<i>t</i>	15379.221566 (21)	21 R R75 (10-7) -70 MHz 3%
15406.9515	P102 (7-5)	<i>t</i>	15406.937545 (27)	15 U (<i>d,e</i>) (<i>f,g</i>) (<i>p,q</i>) R50 (10-7) +560 MHz 5%
15411.4059	R94 (5-4)	<i>t</i>	15411.389346 (27)	15 U (<i>d,e</i>) (<i>f,g</i>) (<i>p,q</i>)
15427.3234	P77 (5-4)	<i>t</i>	15427.306474 (22)	21 U (<i>p,q</i>)
15476.0688	P55 (7-5)	<i>t</i>	15476.051750 (24)	21 R
15524.1299	P89 (6-4)	<i>t</i>	15524.112357 (23)	21 U (<i>p,q</i>)
15575.1479	R56 (6-4)	<i>t</i>	15575.137259 (21)	15 U (<i>d,e</i>) (<i>f,g</i>)

15627.0467	P95 (7-4)	<i>t</i>	15627.030692 (25)	21 U (<i>p,q</i>)
15672.5341	P65 (7-4)	<i>t</i>	15672.517398 (22)	21 R
15727.5394	R22 (9-5)	<i>t</i>	15727.518573 (23)	15 U (<i>f,g</i>) (<i>o,p</i>)
				P16 (9-5) +740 MHz 65%
15758.9686	R89 (8-4)	<i>t</i>	15758.949917 (19)	21 U (<i>p,q</i>)
---	P33 (6-3)	<i>r</i>	15797.967821 (23)	21 R
15807.2941	R50 (8-4)	<i>t</i>	15807.267682 (20)	15 U (<i>d,e</i>) (<i>f,g</i>)
				P44 (8-4) +410 MHz 70%
				P115 (9-4) +520 MHz 25%
				R20 (6-3) +760 MHz 10%
15846.3960	P96 (9-4)	<i>t</i>	15846.384979 (22)	15 U (<i>d,e</i>) (<i>f,g</i>) (<i>p,q</i>)
15856.9424	R96 (9-4)	<i>t</i>	15856.931277 (20)	15 U (<i>d,e</i>) (<i>f,g</i>) (<i>p,q</i>)
15886.5111	P61 (7-3)	<i>t</i>	15886.494949 (24)	21 R
15919.8992	R48 (9-4)	<i>t</i>	15919.884050 (23)	15 U (<i>d,e</i>) (<i>f,g</i>)
15954.0339	R97 (8-3)	<i>t</i>	15954.016985 (24)	21 U (<i>p,q</i>)
				R146 (11-4) -160 MHz 15%
15973.6499	R91 (10-4)	<i>t</i>	15973.631183 (30)	21 U (<i>p,q</i>)
16038.2085	R36 (10-4)	<i>t</i>	16038.192673 (21)	15 U (<i>d,e</i>) (<i>f,g</i>)
16052.4447	R103 (9-3)	<i>t</i>	16052.429625 (19)	21 U (<i>p,q</i>)
				R97 (7-2) -200 MHz 10%

16090.5320	P75 (9-3)	<i>t</i>	16090.515101 (25)	21 R
16130.0815	R47 (9-3)	<i>t</i>	16130.062709 (23)	21 R
16172.3266	P91 (10-3)	<i>t</i>	16172.309240 (23)	21 U (<i>p,q</i>)
16205.9611	R76 (10-3)	<i>t</i>	16205.946017 (20)	15 U (<i>d,e</i>) (<i>f,g</i>) (<i>p,q</i>) R78 (12-4) -650 MHz 20%
16254.6514	P17 (10-3)	<i>t</i>	16254.623391 (23)	21 W P26 (12-4) +240 MHz 20%
16304.5153	P76 (11-3)	<i>t</i>	16304.499027 (31)	15 U (<i>d,e</i>) (<i>f,g</i>) (<i>p,q</i>)
16339.7841	R48 (9-2)	<i>t</i>	16339.768615 (36)	15 U (<i>d,e</i>) (<i>f,g</i>)
16340.6383	R47 (9-2)	<i>i</i>	16340.658054 (31)	21 R P48 (11-3) -700 MHz 170%
16341.7580	R40 (9-2)	<i>t</i>	16341.742422 (20)	15 U (<i>d,e</i>) (<i>f,g</i>) (<i>o,p</i>) (<i>q,r</i>)
16394.6975	P84 (10-2)	<i>t</i>	16394.681360 (27)	15 U (<i>d,e</i>) (<i>f,g</i>) (<i>p,q</i>)
16404.6432	P78 (10-2)	<i>t</i>	16404.626597 (30)	15 U (<i>d,e</i>) (<i>f,g</i>) (<i>p,q</i>)
16424.4665	R70 (10-2)	<i>t</i>	16424.450522 (23)	15 U (<i>d,e</i>) (<i>f,g</i>) (<i>p,q</i>)
16452.4119	R44 (10-2)	<i>t</i>	16452.395097 (23)	15 U (<i>d,e</i>) (<i>f,g</i>) P176 (13-2) +540 MHz 5%
16502.8340	P82 (13-3)	<i>t</i>	16502.817062 (21)	15 U (<i>d,e</i>) (<i>f,g</i>) (<i>p,q</i>) P69 (17-5) +450 7%
16516.8633	R80 (11-2)	<i>t</i>	16516.846551 (24)	15 U (<i>d,e</i>) (<i>f,g</i>) (<i>p,q</i>)

16568.2732	P27 (11-2)	<i>t</i>	16568.255050 (23)	21 W P16 (9-1) +320 MHz 4%
16569.9911	P24 (11-2)	<i>t</i>	16569.974576 (25)	15 U (<i>d,e</i>) (<i>f,g</i>) (<i>o,p</i>) (<i>q,r</i>)
16624.9391	R78 (12-2)	<i>t</i>	16624.923159 (25)	15 U (<i>d,e</i>) (<i>f,g</i>) (<i>p,q</i>)
16638.0457	R69 (12-2)	<i>i</i>	16638.049703 (23)	21 U (<i>p,q</i>) P117 (13-2) +68 MHz 45% R156 (14-2) -590 MHz 20%
16686.0552	P96 (13-2)	<i>t</i>	16686.039067 (21)	15 U (<i>d,e</i>) (<i>f,g</i>) (<i>p,q</i>)
16745.5928	R66 (13-2)	<i>t</i>	16745.576624 (30)	15 U (<i>d,e</i>) (<i>f,g</i>)
16762.1363	R52 (13-2)	<i>t</i>	16762.120059 (21)	15 U (<i>d,e</i>) (<i>f,g</i>)
16780.8572	P26 (11-1)	<i>t</i>	16780.840058 (24)	15 U (<i>d,e</i>) (<i>f,g</i>) (<i>o,p</i>) (<i>q,r</i>) R169 (16-2) +730 MHz 50%
16806.6446	R95 (12-1)	<i>t</i>	16806.627895 (28)	21 U (<i>p,q</i>) P187 (15-1) +620 MHz 7%
16833.1260	R80 (12-1)	<i>t</i>	16833.109663 (46)	15 U (<i>d,e</i>) (<i>f,g</i>) (<i>p,q</i>)
16875.1260	P106 (13-1)	<i>t</i>	16875.109221 (26)	15 U (<i>d,e</i>) (<i>f,g</i>) (<i>p,q</i>)
16891.0383	P18 (12-1)	<i>t</i>	16891.022622 (35)	15U (<i>f,g</i>) (<i>o,p</i>)
16917.3476	P80 (15-2)	<i>t</i>	16917.332049 (20)	15 U (<i>d,e</i>) (<i>f,g</i>) (<i>p,q</i>)
16951.6035	R70 (13-1)	<i>t</i>	16951.597697 (54)	15 U (<i>d,e</i>) (<i>f,g</i>) (<i>p,q</i>) R103 (18-3) -680 1%

17006.0615	R97 (14-1)	<i>t</i>	17006.044184 (24)	21 U (<i>p,q</i>)
17015.0613	P80 (16-2)	<i>t</i>	17015.045402 (22)	15 U (<i>d,e</i>) (<i>f,g</i>) (<i>p,q</i>)
				P50 (20-4) -40 MHz 10%
				P6 (22-4) -1100 MHz 2%
17016.1395	P87 (14-1)	<i>t</i>	17016.122831 (19)	21 U (<i>p,q</i>)
17016.8724	P79 (16-2)	<i>t</i>	17016.856207 (19)	21 U (<i>p,q</i>)
17018.0566	P86 (14-1)	<i>t</i>	17018.039997 (31)	15 U (<i>d,e</i>) (<i>f,g</i>) (<i>p,q</i>)
17018.6605	P78 (16-2)	<i>t</i>	17018.644771 (20)	15 U (<i>d,e</i>) (<i>f,g</i>) (<i>p,q</i>)
				P90 (12-0) -60 MHz 25%
				P47 (20-4) -1360 MHz 25%
17021.8254	P84 (14-1)	<i>t</i>	17021.809376 (19)	15 U (<i>d,e</i>) (<i>f,g</i>) (<i>p,q</i>)
17026.8345	R78 (16-2)	<i>t</i>	17026.818913 (28)	15 U (<i>d,e</i>) (<i>f,g</i>) (<i>p,q</i>)
17029.1037	P80 (14-1)	<i>t</i>	17029.088451 (19)	15 U (<i>d,e</i>) (<i>f,g</i>) (<i>p,q</i>)
17030.4320	P123 (15-1)	<i>t</i>	17030.415189 (25)	21 U (<i>p,q</i>)
17038.3948	P66 (16-2)	<i>t</i>	17038.378860 (33)	15 U (<i>d,e</i>) (<i>f,g</i>) (<i>p,q</i>)
17045.9627	R122 (15-1)	<i>t</i>	17045.945455 (23)	15 U (<i>d,e</i>) (<i>f,g</i>) (<i>p,q</i>)
				P85 (21-4) +480 MHz 15%
17048.0993	R64 (16-2)	<i>t</i>	17048.083923 (25)	15 U (<i>d,e</i>) (<i>f,g</i>) (<i>p,q</i>)
17049.2328	P116 (15-1)	<i>t</i>	17049.217506 (53)	15 U (<i>d,e</i>) (<i>f,g</i>) (<i>p,q</i>)
17099.3577	P86 (17-2)	<i>t</i>	17099.342383 (20)	15 U (<i>d,e</i>) (<i>f,g</i>) (<i>p,q</i>)

17101.1754	P94 (15-1)	<i>t</i>	17101.180948 (21)	15 U (<i>d,e</i>) (<i>f,g</i>) (<i>p,q</i>)
17123.3262	P73 (17-2)	<i>t</i>	17123.309988 (29)	21 U (<i>p,q</i>)
				P31 (21-4) +550 MHz 15%
17144.3553	R64 (17-2)	<i>t</i>	17144.338765 (27)	15 U (<i>d,e</i>) (<i>f,g</i>) (<i>p,q</i>)
				R83 (22-4) -980 MHz 5%
				P171 (18-1) -1100 MHz 5%
17157.4114	R67 (15-1)	<i>t</i>	17157.396892 (28)	21 U (<i>p,q</i>)
17166.0191	P108 (16-1)	<i>t</i>	17166.002813 (23)	15 U (<i>d,e</i>) (<i>f,g</i>) (<i>p,q</i>)
				P67 (32-4) +90 MHz 5%
17194.9067	R30 (15-1)	<i>t</i>	17194.891763 (29)	15 U (<i>d,e</i>) (<i>f,g</i>)
17199.8446	R98 (16-1)	<i>t</i>	17199.827846 (21)	15 U (<i>d,e</i>) (<i>f,g</i>) (<i>p,q</i>)
17205.8047	P98 (14-0)	<i>t</i>	17205.788933 (28)	15 U (<i>d,e</i>) (<i>f,g</i>) (<i>p,q</i>)
				R140 (15-0) -60 MHz 40%
17252.0411	P74 (14-0)	<i>t</i>	17252.023212 (21)	15 U (<i>d,e</i>) (<i>f,g</i>) (<i>p,q</i>)
				R105 (19-2) +160 MHz 50%
17300.0056	P12 (16-2)	<i>t</i>	17299.991091 (48)	15 R
				R168 (22-2) -550 MHz 2%
17349.6773	R80 (15-0)	<i>t</i>	17349.661322 (24)	15 U (<i>d,e</i>) (<i>f,g</i>) (<i>p,q</i>)
17352.2451	P62 (17-1)	<i>t</i>	17352.231328 (28)	15 U (<i>d,e</i>) (<i>f,g</i>) (<i>p,q</i>)

17360.6176	P56 (17-1)	<i>t</i>	17360.601438 (34)	15 U (<i>d,e</i>) (<i>f,g</i>) P149 (22-2) -410 MHz 2%
17380.8317	P38 (17-1)	<i>t</i>	17380.816923 (21)	15 U (<i>d,e</i>) (<i>f,g</i>)
17405.1703	R90 (18-1)	<i>t</i>	17405.154995 (31)	15 U (<i>d,e</i>) (<i>f,g</i>) (<i>p,q</i>) ^d
17448.3784	R42 (20-2)	<i>t</i>	17448.363077 (24)	15 U (<i>d,e</i>) (<i>f,g</i>)
17450.7924	R78 (16-0)	<i>t</i>	17450.775435 (39)	15 U (<i>d,e</i>) (<i>f,g</i>) (<i>p,q</i>)
17461.1972	P67 (16-0)	<i>t</i>	17461.182208 (29)	21 U (<i>p,q</i>)
17500.8423	R88 (19-1)	<i>t</i>	17500.827932 (42)	15 U (<i>d,e</i>) (<i>f,g</i>) (<i>p,q</i>)
17501.1370	R38 (16-0)	<i>t</i>	17501.121870 (26)	15 U (<i>d,e</i>) (<i>f,g</i>) P70 (29-5) -500 MHz 15%
17521.7500	R77 (19-1)	<i>t</i>	17521.737626 (26)	21 U (<i>p,q</i>)
17531.3938	P67 (19-1)	<i>t</i>	17531.384093 (22)	21 U (<i>p,q</i>)
17550.0663	R76 (17-0)	<i>t</i>	17550.050483 (53)	15 U (<i>d,e</i>) (<i>f,g</i>) (<i>p,q</i>) P125 (26-3) -350 MHz 15%
17578.5963	P26 (19-1)	<i>i</i>	17578.599454 (22)	15 U (<i>d,e</i>) (<i>f,g</i>) R92 (25-3) -840 MHz 30%
17605.3257	P23 (17-0)	<i>t</i>	17605.308074 (29)	21 W
17609.8910	R18 (17-0)	<i>t</i>	17609.875064 (36)	15 U (<i>f,g</i>) (<i>q,r</i>) P159 (23-1)? +430 MHz 30%
17655.9473	P42 (20-1)	<i>t</i>	17655.932802 (41)	15 U (<i>d,e</i>) (<i>f,g</i>)

17668.6723	R32 (20-1)	<i>t</i>	17668.657200 (29)	15 U (<i>d,e</i>) (<i>f,g</i>)
17685.4130	R46 (18-0)	<i>t</i>	17685.398042 (22)	15 U (<i>d,e</i>) (<i>f,g</i>)
17704.6867	R19 (18-0)	<i>t</i>	17704.669058 (20)	21 W
17742.5173	R68 (19-0)	<i>t</i>	17742.501454 (22)	15 U (<i>d,e</i>) (<i>f,g</i>) (<i>p,q</i>)
17811.1027	R84 (20-0)	<i>t</i>	17811.087494 (21)	15 U (<i>d,e</i>) (<i>f,g</i>) (<i>p,q</i>)
				R49 (27-3) -100 MHz 20%
17845.2272	P28 (22-1)	<i>t</i>	17845.202199 (20)	15 R
				R32 (22-1) +390 MHz 100%

^a Ref. 1 with correction of Ref. 2.

^b The uncertainty in parentheses represents a 95% confidence interval.

^c The first comment line contains:

- The number of hyperfine components.

- A code describing the hyperfine structure as follows:

R = fully resolved

U = not all components resolved

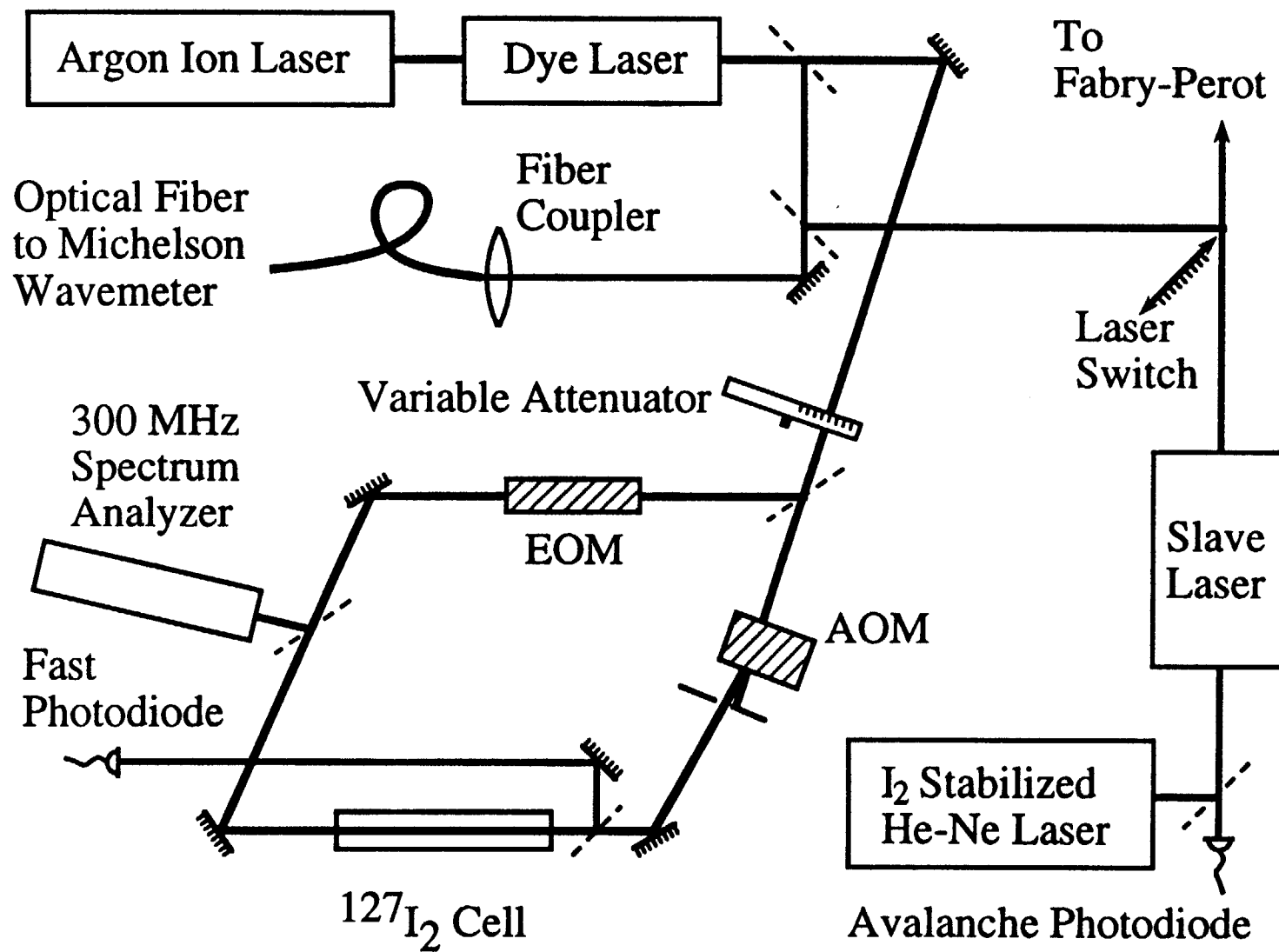
W = widely distributed structure without 6 clear groups of components.

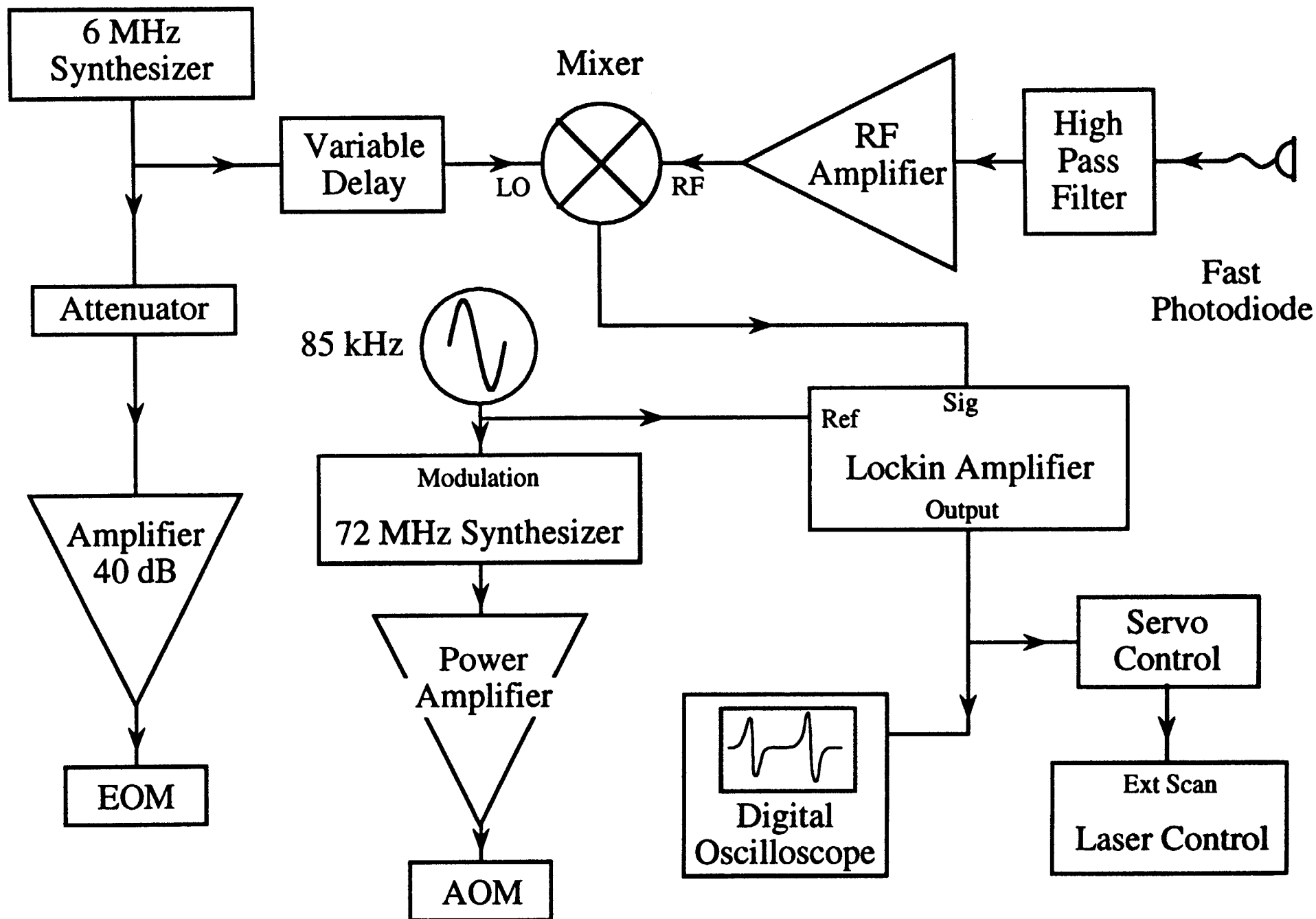
- A list of pairs of components that were not resolved under our experimental conditions.

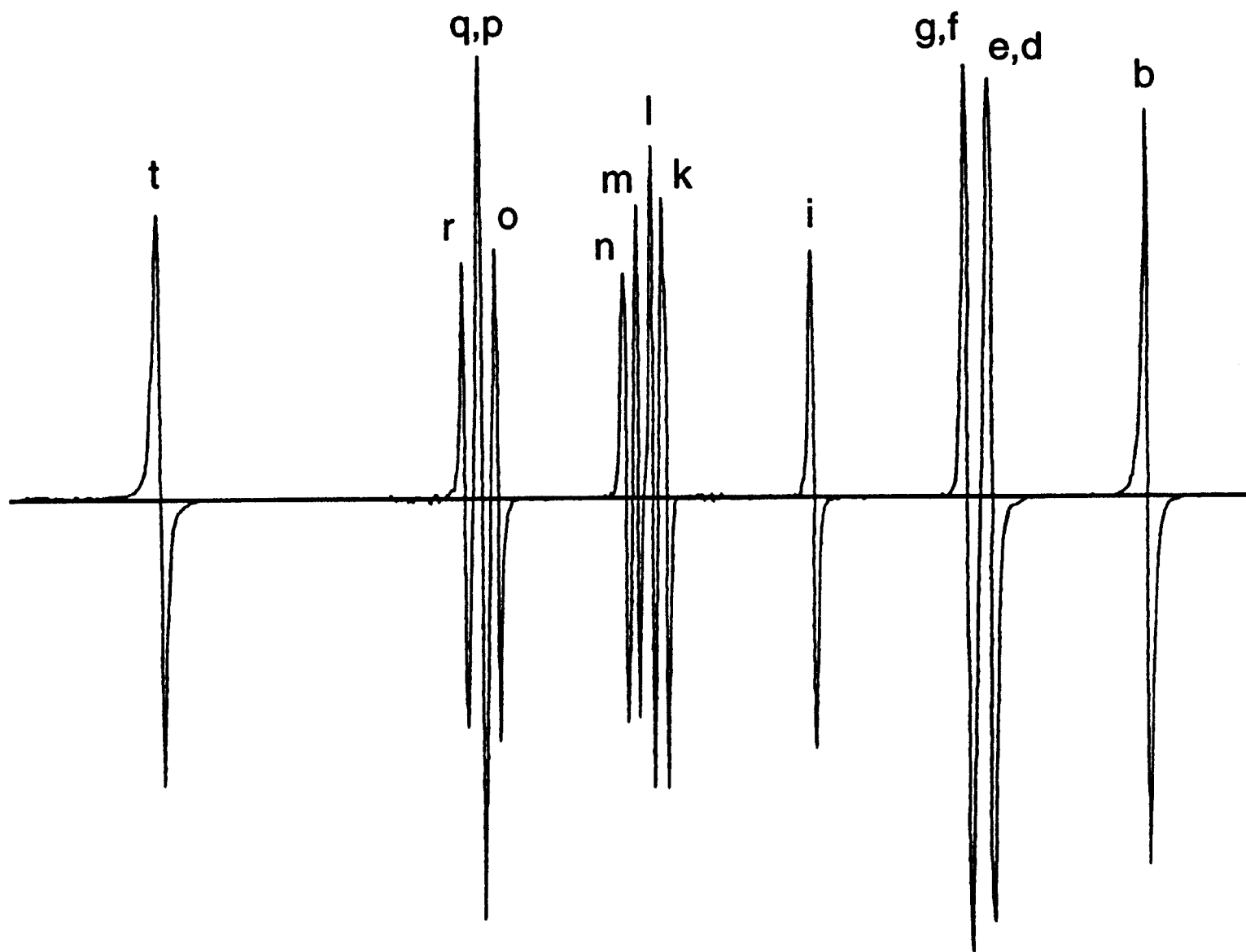
Additional comment lines are present only if components of another transition were observed in the same laser scan with the transition of interest. Each additional line contains:

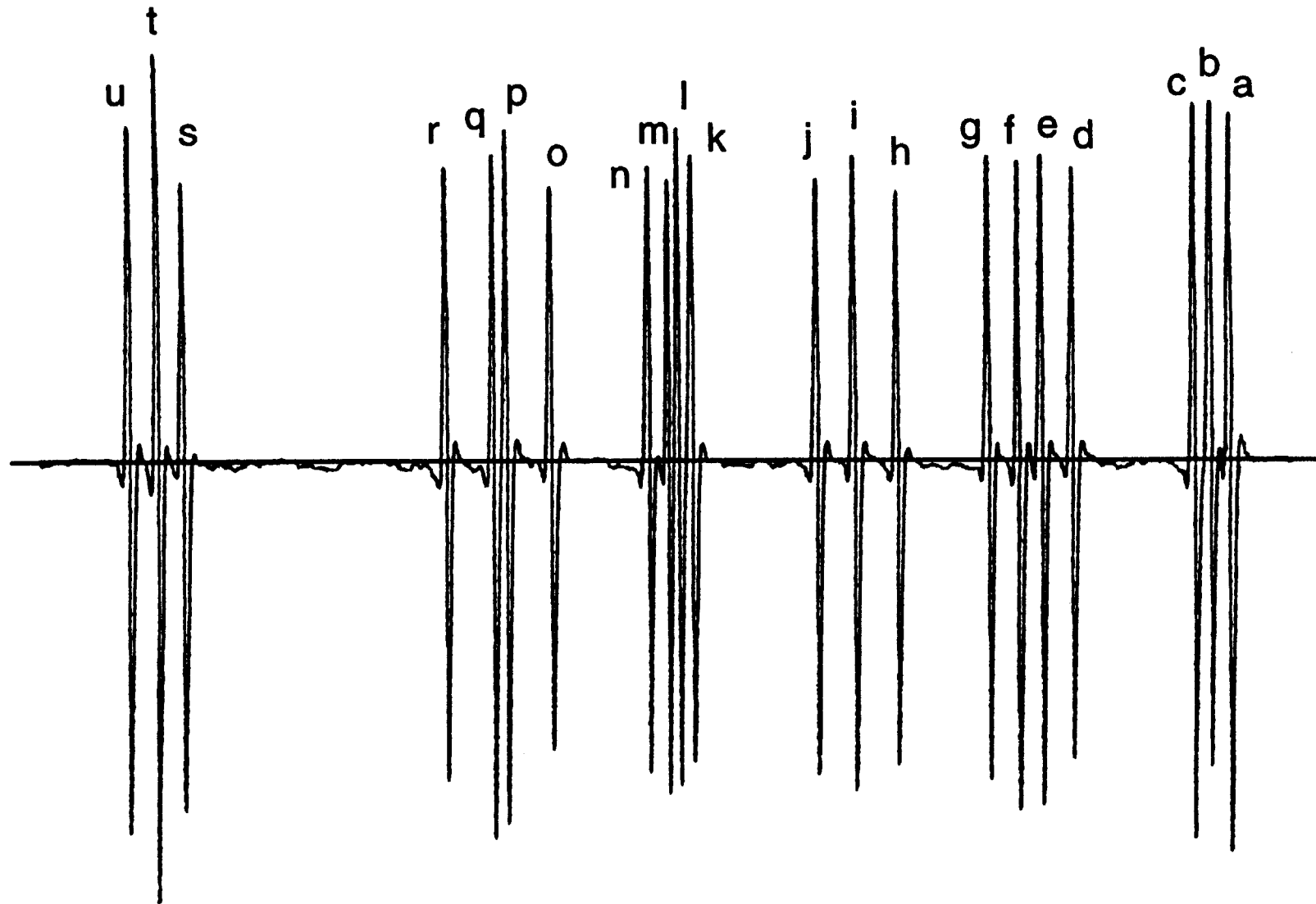
- The classification of the overlapping or adjacent transition.
- An estimate of the offset between the centers of gravity of the transition of interest and the overlapping transition.
- A rough estimate of the strength of the overlapping transition as a percentage of the transition of interest.

^d Recorded scan not available for this transition. Calculations show no adjacent or overlapping lines. Inspection of other transitions in this band indicate that these are the likely unresolved components.

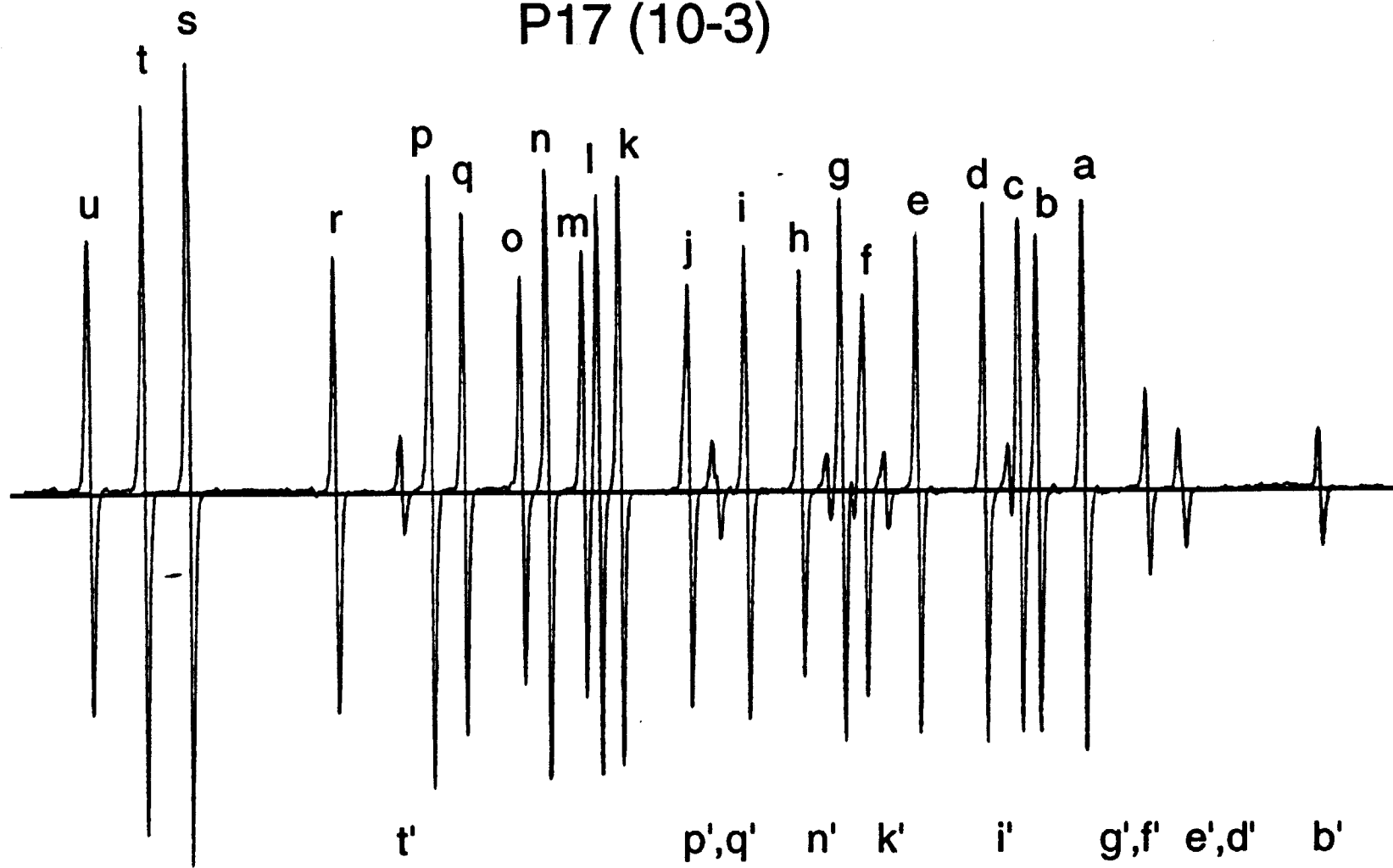




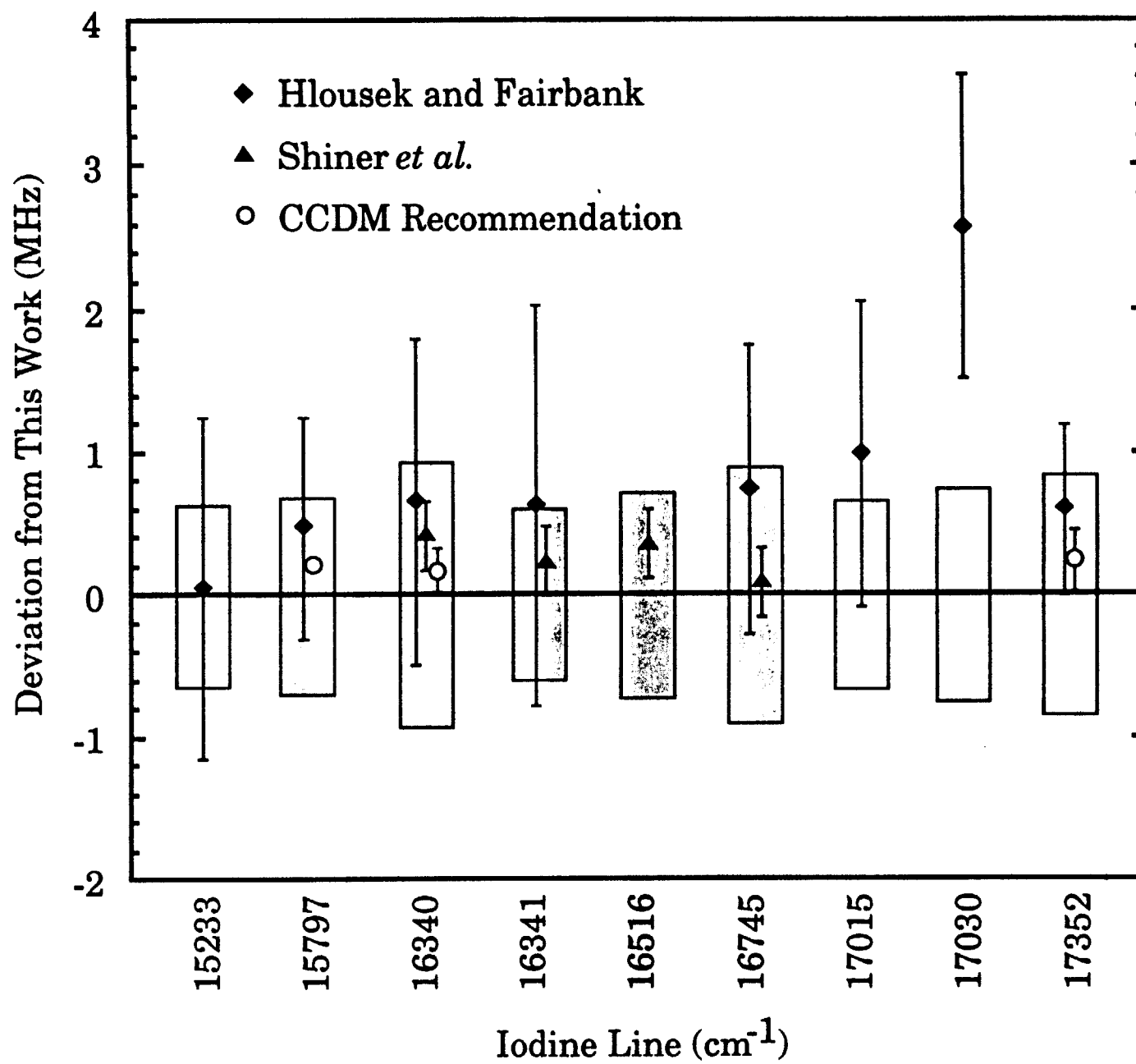


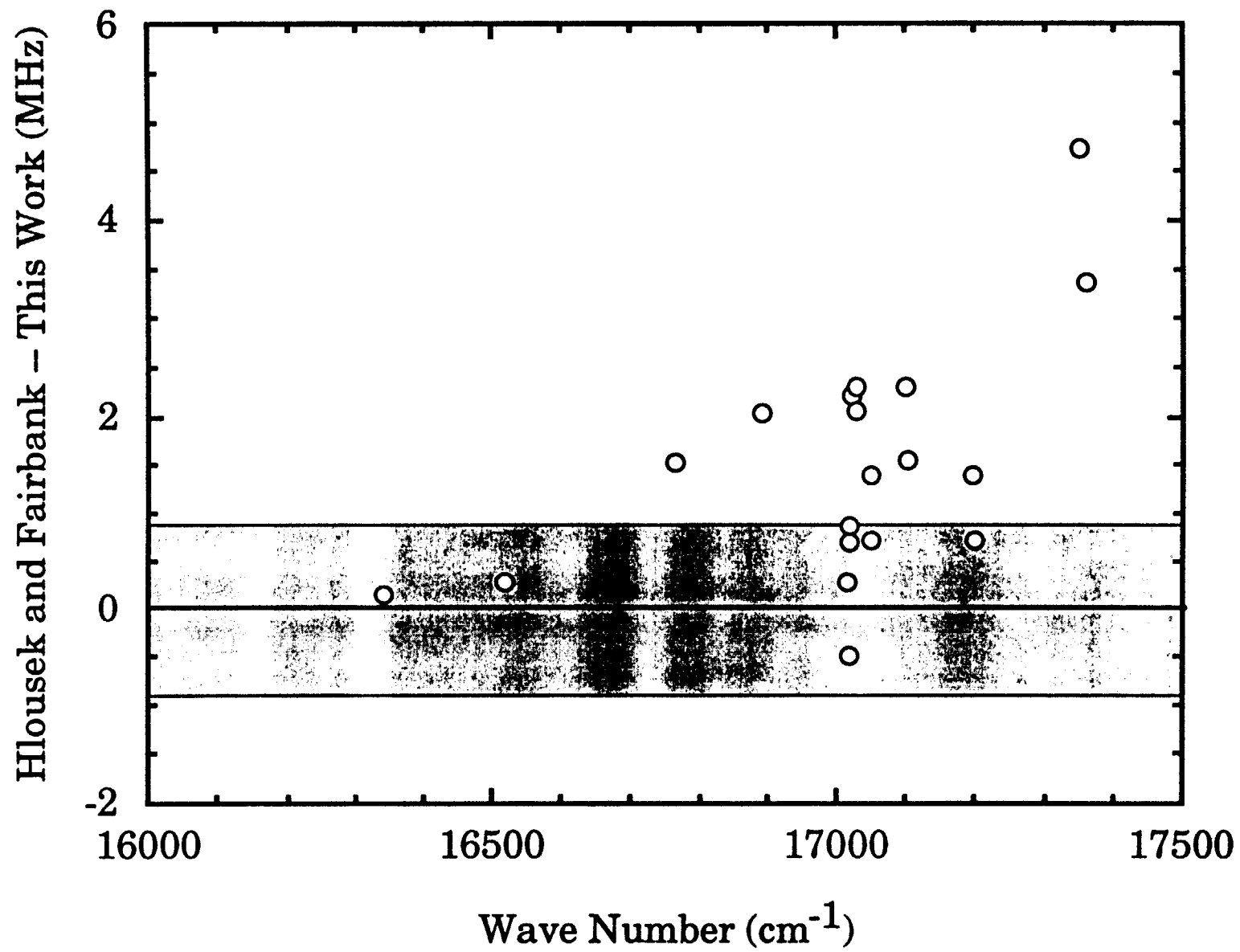


P17 (10-3)



P26 (12-4)





Technical Information Department • Lawrence Livermore National Laboratory
University of California • Livermore, California 94551

